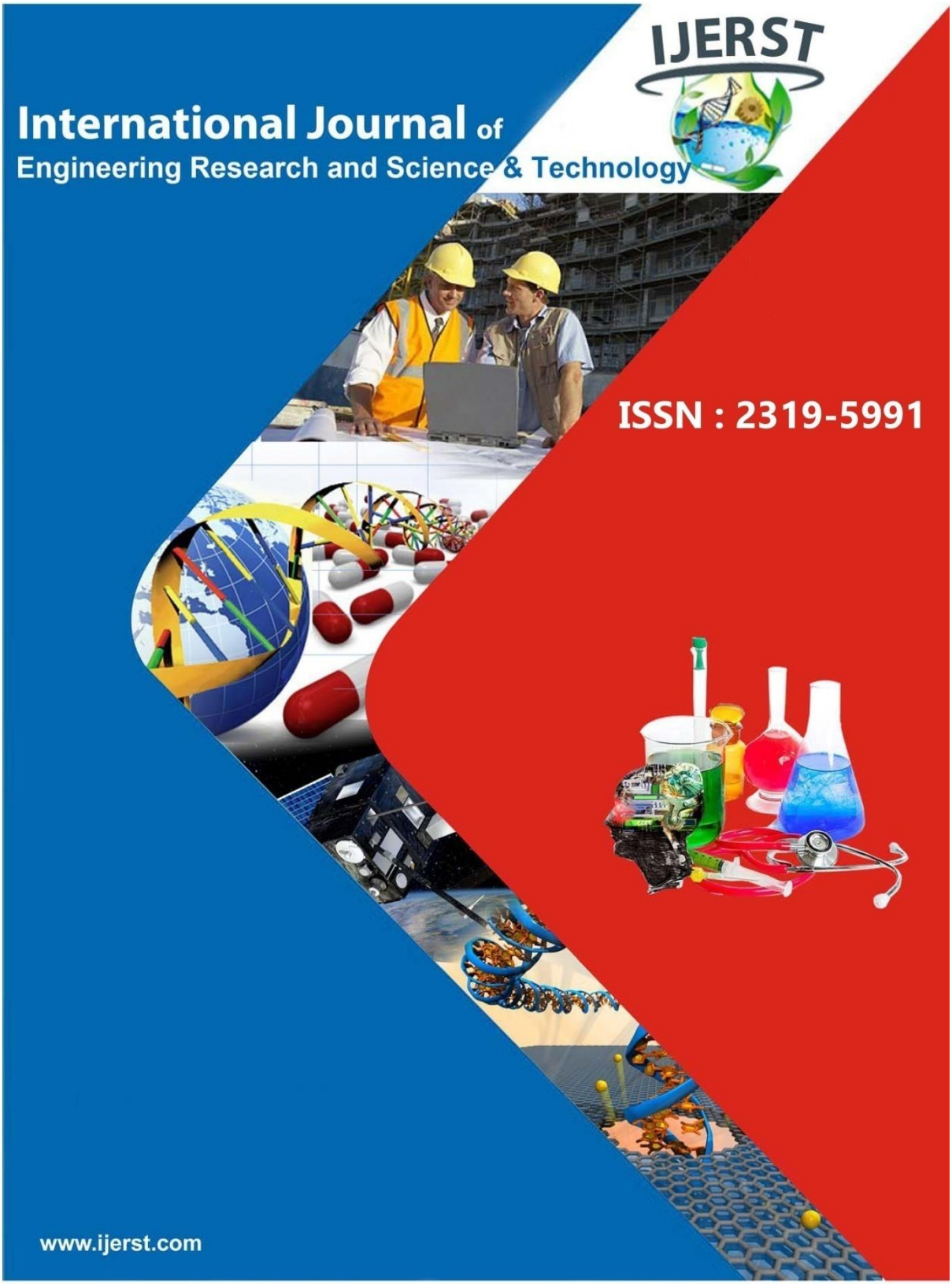

Email: editor@ijerst.com or editor.ijerst@gmail.com

International Journal of Engineering Research and Science & Technology

ISSN 2319-5991 www.ijerst.com
Vol. 10, Issuse.3,Sep 2022

OPTIMIZATION OF THE THICKNESS OF THE SUB-BASE LAYERS OF FLEXIBLE PAVEMENTS BASED ON LATERITIC GRAVEL OF AVLAMÈ IMPROVED WITH GRANITE CRUSHED STONE

Kocouvi Agapi Houanou , Kpomagbé Serge Dossou, Judicaël Agbélélé, Vincent Prodjinonto and Emmanuel Olodo

Abstract

The exploitation of raw or improved lateritic gravel in road construction is of major interest. Such is the case of the lateritic gravel of Avlamè improved with granite crushed of Dan 0/31.5 usable in road construction in Benin. In this perspective, the present study is initiated to investigate the influence of elastic (E=5CBR) and secant moduli in the determination of pavement base layer thicknesses. A comparative study was carried out by considering the elastic and secant moduli for the design of several pavement variants using the Alizé software of LCPC-SETRA. The results obtained show that the use of the secant modulus for the design allows a reduction in the thickness of the base course of 20% and 13.33% respectively for the variants V1 and V2. As for the variants V3 and V4, no reduction is observed. Moreover, the use of the secant modulus for the design of the subgrade allows a reduction of 25% in the thickness of each of these variants compared to the use of the elastic modulus. Also, the secant modulus allows to reduce the thickness of the base course by 16.67% and 13.33% respectively for the variants V5 and V6, and by 23.08% for the variants V7 and V8 compared to the use of the elastic modulus (5CBR). As for the design of the subbase layers, the use of the secant modulus allows to reduce the thickness of the subbase layers by 13.33 %, whatever the variant (V5 to V8), compared to the use of the elastic modulus. These results show that the thickness of the pavement structure decreases with increasing moduli (E=5CBR and E50).

Key words: lateritic gravel of Avlamè, secant modulus, elastic modulus, subgrade, base course

Introduction

For decades, in the world and particularly in sub-Saharan Africa, large quantities of lateritic gravel have been used in road construction. This large consumption of the said material by road construction projects leads to the depletion of the available reserves, despite their quantitative importance. To compensate the lack of good quality lateritic gravel, technical solutions of improvement of the lateritic gravel of lesser quality are put to contribution. This is the case of the lateritic gravel of Avlamè, which studies have shown that it cannot be used exclusively in sub-base layers in its natural state (Houanou et al. 2022a).

University of Abomey-Calavi, Polytechnic School of Abomey-Calavi, Laboratory of Energetic and Applied Mechanic, Abomey-Calavi, Republic of Benin.
National University of Science Technology Engineering and Mathematics (UNSTIM), Abomey, Republic of Benin
E-mail : agapikh13@yahoo.fr

Thus, to use it fully in all parts of the pavement body, the litho-stabilization technique was used to enhance its technical qualities (Houanou et al. 2022b). Indeed, litho-stabilization consists in improving the bearing capacity or the resistance of lateritic gravels used in sub-base layers by adding a quantity of crushed stone determined later (Nassir 2015; Babaliyè et al. 2020; Ahouétohou et al. 2021; Houanou et al. 2022b).

The materials developed in this way will be used in the design and dimensioning of the pavement structures to be projected. Pavement design provides technically, economically and environmentally feasible structures. From a social point of view, the design and construction of a road allow the optimization of the level of service offered to users. To this end, it is important to combine the thicknesses of the layers and the quality of the constituent materials, so that they adapt to the traffic and environmental conditions, maintaining reasonable costs in both the construction and operation phases.The present study is initiated to optimize the thickness of flexible pavement sub-base layers from raw or improved lateritic gravel of Avlamè to granite crushed rock of Dan 0/31.5 (Houanou et al. 2022b). In order to investigate the influence of the input parameters, E50 and E=5CBR, a comparative study was carried out based on the values of the calculated thicknesses of the different subgrade layers and their deformation meeting the admissibility criteria.

Materials and methods

Material

Presentation of the study area

The road targeted in this study is the one that connects the villages of Ouèdo, in the commune of Abomey-Calavi, and Tori-Bossito, in the commune of Tori-Bossito, all located in the Atlantic Department (Republic of Benin). Its length is 15.50 km (Colas Afrique, 2021). Figure 1 shows the route of the targeted road.

On this road, the average annual daily traffic (AADT) is 109 HGV/day with a geometric growth rate equal to 5% (Colas-Afrique, 2021), corresponding to traffic class T3 according to the CEBTP guide (1984). The initial service life of the pavement is taken equal to 15 years corresponding to the time required before the appearance of the first pavement distresses in accordance with the recommendations of the CEBTP (1984) and CEBTP (2019) guides. According to the CEBTP (2019) guide, the risk of overloading by heavy vehicles is taken between 10% and 20%. Thus, this design risk is taken equal to 10% in this study. In addition, the CEBTP (1984) guide recommends limiting the weight per axle to 13 tons.

The subgrade of the targeted road has a CBR of 20% (Colas Afrique, 2021). Thus, its elastic modulus is 100 MPa at the surface of the subgrade (CEBTP 1984, 2019; NF P98-086 2019). Therefore, the road subgrade is of type PF2+ according to NF P98-086 (2019) with a coefficient ks = 1/1.065. The Poisson's ratio of the supporting soil is υ = 0.35 according to the current standards (CEBTP 1984, 2019; NF P98-086 2019).

Materials

The materials used in this study are those developed from the lateritic gravel of Avlamè and the granitic crushed stone of Dan 0/31.5 (Houanou et al. 2022a, b, c: under press). They are: Mixture M0 (100GL+0%CG), Mixture M1 (90%GL+10%CG), Mixture M2 (85%GL+15%CG), Mixture M3 (80%GL+20%CG), Mixture M4 (75%GL+25%CG), Mixture M5

(70%GL+30%CG) and Mixture M6 (65%+35%CG). The mechanical design characteristics of these different materials are shown in Table 1 below:

The Poisson's ratio for unbound granular materials is $\upsilon = 0.35$ according to current standards (CEBTP 1984, 2019; AGEROUTE-Sénégal 2015; NF P98-086 2019).

As for the average aggressiveness coefficient (CAM), it is recommended to take 2 for unbound materials (SETRA-LCPC 1998a, b; NF P98-086 2019). The interfaces between the layers are bonded (SETRA-LCPC 1998a).

Concerning the bituminous materials, the characteristics used during the dimensioning are recorded in the Alizé software of LCPC-SETRA versions 231.

Method

The design of a pavement structure consists in evaluating the thickness of each of its layers. It starts from the evaluation of the stress level of the structure to determine the thicknesses of the different layers of the pavement in order to limit the stresses and strains to values lower than those admissible for a given traffic (SETRA-LCPC 1998a; Fall et al. 2002; Alizé 2003, 2021; Kimbonguila et al. 2015). The sizing is done using the Alizé 3: 2003 software according to the procedure described below.

Step 0: Define basic assumptions;

Step 1: Choose the type of structure, materials and layer thicknesses;
The pavement structure highlighted in this study is a flexible pavement structure. Figure 2 shows the typical flexible pavement structure.

The selected pavement structure is composed of a base course (sub-base course and base course) resting on a subgrade and a wearing course (binder course in asphalt gravel and bituminous concrete). This type of structure is chosen to reduce the rapid deterioration of the subbase layers. This pavement structure is similar to those proposed in the CEBTP guide (1984), by the NF P98-086 standard (2019), by Srikanth (2015).

Table 2 shows the materials and layer thicknesses for the different variants of the typical pavement structure.

Step 2: Calculate the maximum traffic loads in the different layers;

Step 3: Calculate the allowable stresses in the different layers;

Step 4: Comparison of (Step 2) and (Step 3), between the maximum stresses generated in the structure and the stresses considered admissible;

Step 5: Possible adjustment of the layer thicknesses to respect the admissible stress.

Results and discussions

The results of the design of the different projected variants and the verifications are presented in the following sections. They are developed in two parts depending on the type of modulus used, either the elastic modulus from the CBR approximation (CEBTP 1984) or the experimentally determined secant modulus.

Thickness values determined by considering the elastic modulus (5CBR)

Table 3 presents the pavement design results, the thickness of the different layers, for each pavement structure variant.

From the analysis of Table 3, it appears that the thickness of each structure decreases with the increase of the elastic modulus. In fact, from variant V1 to V4, it varies from

56.00 cm to 46.00 cm with a sub-base layer in raw lateritic gravel while from variant V5 to V8, it goes from 49.00 cm to 44.00 cm with a sub-base layer in lateritic gravel improved with 10% granitic crushed stone. These results are similar to those found by Elshamey et al. (2021). Figure 4 shows the evolution of the pavement thicknesses according to the pavement structure variant.

From the analysis of Figure 4 (a), it can be seen that the thickness of the base layer decreases as the elastic modulus increases. However, it is noted that the thickness of the base layer becomes constant from variant V3 onwards.

Similarly, Figure 4 (b) shows the same observation trend as Figure 4 (a). In this case, the thickness of the base course is constant from variant V7 onwards. From this figure 4, it can be seen that the improvement of the granite crushed base layer dosed at 10% allows to reinforce the structure of the said layer and to increase its mechanical capacity. Thus, there is an overall reduction in the thickness of the pavement structure.

Figure 5 shows the evolution of the elastic modulus as a function of the pavement structure thickness.

From the analysis of Figure 5, it can be seen that the pavement base layer thickness decreases with increasing elastic modulus to stabilize from the value of elastic modulus equal to 503.33 MPa. These observations are similar to those found by Srikanth (2015), by Elshamey et al. (2021).

Value of the elastic deformation of the layers of each pavement structure variant

The results of the design are presented in Table 4.

From the analysis of Table 4, it appears that the deformations at the base of each of the asphalt concrete and gravel layers are lower than the permissible values of deformations recommended respectively by the standards (CEBTP 1984; AGEROUTE-Sénégal 2015; NF P98-086 2019).

As for the vertical deformations at the surface of each of the base layers of each pavement variant, they vary in a sawtooth pattern from 478.30 μdef, 437.80 μdef, 718.80 μdef, 398.40 μdef, 478.10 μdef, 437.50 μdef, 419.90 μdef, and 399.10 μdef for each of the pavement structure variants V1, V2, V3, V4, V5, V6, V7, and V8, respectively. Similarly, the vertical deformations at the surface of each of the subgrade layers vary from 252.80 μdef to 397.80 μdef while the vertical deformations at the subgrade surface vary from 387.70 μdef to 495.00 μdef. However, it can be seen that the deformations evolve in a sawtooth pattern. All these values, obtained from the vertical deformation, are lower than the admissible values of deformations recommended respectively by the standards (CEBTP 1984; AGEROUTE-Sénégal 2015; NF P98-086 2019). These results are in line with the current normative recommendations and previous works (Subagio et al. 2005; IDRRIM 2017; T50 2019; Elshamy et al. 2021; Tiraturyan et al. 2021).

Thickness values determined from the secant modulus (E_{50})

Table 5 presents the pavement design results considering the secant modulus.

Table 5 shows the decrease in thickness of each structure with the increase of the secant modulus. Indeed, from variant V1 to V4, we observe a decrease in thickness from 47.00 cm to 41.00 cm with a sub-base of crushed lateritic gravel. Similarly, from variant V5 to V8, the thickness decreases from 44.00 cm to 39.00 cm with a sub-base made of lateritic gravel improved with 10% granite crushed stone. Figure 6 shows the evolution of the pavement thicknesses according to the variant.

Figure 6 (a) shows the evolution of the thicknesses of the pavement base layers (base layer + subbase layer) according to the pavement variant. A decrease of the base layer is observed with the increase of the secant modulus until its stabilization from the V3 variant.

Similarly, Figure 6 (b) shows the same trend as Figure 6 (a). However, the thickness of the base layer becomes invariant from variant V7 onwards. Figure 7 shows the evolution of the secant modulus as a function of the pavement structure thickness.

This figure 7 shows the drop in thickness of each of the pavement base layers according to the increase of the secant modulus until its stabilization from 6 774.39 MPa, value of the secant modulus.

Table 6 presents the results of the calculated deformations at the surface of each of the pavement structure layers.

Table 6 above shows that the deformations at the base of each of the asphalt concrete and gravel layers are lower than the permissible values of deformations recommended respectively by the standards (CEBTP 1984; AGEROUTE-Senegal 2015; NF P98-086 2019).

As for the vertical deformations at the surface of each of the base layers of each pavement structure variant, they regress from 182.20 µdef to 12.50 µdef respectively for pavement structure variants V1 to V4 and then from 181.80 µdef to 12.90 µdef respectively for pavement structure variants V5 to V8. It can be seen that the deformations decrease with the increase of the percentage of granite crushed material contained in each mix. All these vertical deformations, obtained at the surface of each of the base layers, are lower than the value of the admissible deformation recommended by the NF P98-086 standard (2019), the CEBTP guide (1984) and revised in 2019 and the AGEROUTE-Senegal catalog (2015).

Similarly, the vertical deformations at the surface of each of the foundation layers range from 144.10 µdef and 243.20 µdef while the vertical deformations at the subgrade surface range from 343.50 µdef to 379.60 µdef. All of these deformations are less than the allowable values.

Parametric study

From the above results, it can be seen that there is a difference between the pavement thicknesses obtained by elastic modulus (5CBR) and those obtained by secant modulus. Figure 8 shows the evolution of the pavement base layer thicknesses as a function of the mixtures.

Figure 8 above shows that the different curves have the same trend of evolution. There is a reduction in the thickness of each of the bedding layers following the mixtures. These results are similar to those obtained by Ratsifarehandahy et al. (2020), by Ahouet et al. (2019), by Dolin et al. (2022), by Kimbonguila, et al. (2015), by Mengue et al. (2015), by Simonin (2002), by Srikanth (2015) and by Elshamey et al. (2021). Table 7 presents the ratio of percentage of rational thicknesses in materials.

Table 7 shows that the use of the secant modulus allows the rationalization of the pavement structure thickness for M0 (100%GL+0%CG) and M1 (90%GL+10%CG) materials.

- Case of material M0 (100%GL+0%CG)

In fact, for the base layer, the use of the secant modulus in the design reduces the thickness of this layer by 20% compared to the use of the elastic modulus (5CBR) for variant V1 and by 13.33% for variant V2. As for the variants V3 and V4, no reduction is observed. Similarly, the dimensioning of the

subgrade layer based on the secant modulus allows a 25% reduction in the thickness of the said layer compared to that calculated by considering the elastic modulus for variants V1 to V4.

- Case of material M1 (90%GL+10%CG)

When considering the variants V5 to V8, the use of the secant modulus in the pavement design with the lateritic gravel of Avlamè improved with 10% of the granitic crushed stone in the sub-base layer, allows a reduction of the base layer of 16.67% and 13.33% respectively at V5 and V6, then a reduction of 23.08% for the variants V7 and V8 compared to the use of the elastic modulus (5CBR). In the sub-base layer, the use of the secant modulus in the design of the pavements allows to reduce the thickness of this layer by 13.33 % for the variants V5 to V8 compared to the use of the elastic modulus.

Conclusion

The present study was initiated with the aim of optimizing the thickness of the sub-base layers of flexible pavements from mixtures of Avlamè lateritic gravel and granite crushed stone of Dan 0/31.5 (Houanou et al. 2022a, b, e: under press). Thus, variants of pavement structures were designed respectively with the secant modulus (E50) and the elastic modulus (5CBR) by the French mechanistic-empirical method, based on the calculation of the Alizé software of LCPC-SETRA versions 231. In total, eight (8) pavement structure variants were modelled and designed. They are grouped into two (2) categories according to the nature of the subgrade material, namely M0 (100%GL+0%CG) and M1 (90%GL+10%CG). The variants V1 to V4 have their sub-base in M0 material while the variants V4 to V8 have a sub-base made of M1.

The results obtained from this study show that the thickness of the pavement structures decreases with increasing modulus (E=5CBR and E50). Although the secant modulus determined for each material is experimental, it allows a reduction in the thickness of the base course of 20% and 13.33% respectively for variants V1 and V2. As for the variants V3 and V4, no reduction is observed. Moreover, the use of the secant modulus in the design of the sub-base layer reduces the thickness of each of these variants by 25% compared to the use of the elastic modulus.

Also, the secant modulus reduces the thickness of the base course by 16.67% and 13.33% respectively for variants V5 and V6, and by 23.08% for variants V7 and V8 compared to the use of the elastic modulus (5CBR). As for the sub-base layer, the use of the secant modulus in the design of the pavements makes it possible to reduce the thickness of this layer by 13.33 %, whatever the variant (V5 to V8), compared to the use of the elastic modulus.

References

AGEROUTE-Sénégal (2015), « Catalogue de structures de chaussées neuves et guide de dimensionnement des chaussées au Sénégal ». Sénégal, AGEROUTE-Sénégal, 214 p.

Ahouet L, ELENGA, and R. Gentil (2019), « Amélioration des propriétés géotechniques du graveleux latéritique par ajout de la grave alluvionnaire concassée 0/31.5 ». Sciences Appliquées et de l'Ingénieur, vol. 3, N° 1, p. 1–6.

Ahouétohou P 2021, « Détermination des caractéristiques mécaniques de la grave latéritique de Avlamè améliorée en vue de son utilisation en construction routière au Bénin ». EPAC/UAC, p. 136.

Alizé (2021), « Documentation utilisateur : Dimensionnement routier et Vérification au gel ». Paris, Université Gustave Eiffel, Alizé, 80 p.

Alizé (2003), « Manuel d'utilisation Alizé-LCPC ». Paris, Université Gustave Eiffel.

Babaliye O, Houanou A, Vianou A, Adolphe T, Erick F (2020), « Litho-stabilization of the lateritic gravelly by granite crushed for their use in flexible pavement in Bénin ». International Journal of Advanced Research, v. 8, p. 1008–1016, doi :10.21474/IJAR01/10871.

CEBTP (1984), « Guide pratique de dimensionnement des chaussées pour les pays tropicaux ».

CEBTP (2019), « Revue du guide pratique de dimensionnement des chaussées pour les pays tropicaux ».

Dolin, R. F., M. Ramaroson, R. Rabevala, and R. J. De (2022), « Comportement mécanique des chaussées souples a l'incorporation du fondu de déchets de sachets plastiques sur la consistance de l'huile lourde de Tsimiroro : application a la prévision de l'orniérage ». Am. J. innov. res. appl. sci., vol. 14, N°2, p. 74–83, doi: Ratsifaherandahy-Ref03-ajira080222.

Elshamy MM, Tiraturyan AN, Uglova EV (2021), « Evaluation of the elastic modulus of pavement layers using different types of neural networks models». Advanced Engineering Research, vol. 21, N° 4, p. 364–375.

Fall M, Senghor B, Lakhoune A (2002), « Analyse de la pratique du dimensionnement rationnel des structures de chaussées au Sénégal. Influence des paramètres d'entrée dans les codes de calcul pour le renforcement des chaussées ». Annales du bâtiment et des travaux publics (Paris), N° 1, p. 5–13.

Houanou KA, Dossou KS, Doko KV, Prodjinonto V, Olodo E (2022), « Engineering characteristics of Avlamè lateritic aggregate for it use in road construction in the Republic of Benin ». Australian Journal of Basic and Applied Sciences, vol. 16, N° 7, p. 8–19, doi: 10.22587/ajbas.2022.16.7.2.

Houanou KA, Dossou KS, Prodjinonto V, Ahouétohou P, Olodo E (2022), « Mechanical characteristics of Avlamè lateritic gravel improved with granite crushed for its use in road construction in Benin ». World Journal of Advanced Research and Reviews, vol. 15, N° 2, p. 279–292, doi:10.30574/wjarr.2022.15.2.0820.

Institut Des Routes, des Rues et des Infrastructures de Mobilité (IDRRIM) (2017), « Guide d'application du fascicule 25 du cahier des clauses des techniques générales (CCTG). Exécution des assises de chaussées en matériaux non traites et traites aux liants hydrauliques ». Paris, Institut Des Routes, des Rues et des Infrastructures de Mobilité (IDRRIM), fascicule 25, 78 p.

Kimbonguila A, BECQUART F, ABRIAK NE (2015), « Méthode de dimensionnement des structures de chaussées : quelle(s) adaptabilité(s) pour les matériaux granulaires alternatifs ? ». I*n* Rencontres Universitaires de Génie Civil, Bayonne, France.

Mengue E, Mroueh H, Lancelot L, Eko RM (2015), « Dimensionnement d'une assise de chaussée à base d'un sol latéritique traité au ciment à différents dosages ». I*n* Rencontres Universitaires de Génie Civil.

Nassir AD (2015), « La litho stabilisation en couche de chaussée : cas de la voirie urbaine de SABANGALI (N'DJAMENA- TCHAD) ». Mémoire : Institut International d'Ingénierie de l'Eau et de l'Environnement., 42 p.

NF P98-086 (2019), « Dimensionnement structurel des chaussées routières-

Application aux chaussées neuves ». AFNOR.

Ratsifarehandahy DF, Ramaroson M, Rabevala R, Richard T (2020), « Etude de la stabilisation de latérite par les liants, végétaux locaux et additif pour la construction routière ». p. 7.

SETRA-LCPC (1998a), « Assises de chaussées-guide d'application des normes pour le réseau routier national ».

SETRA-LCPC (1998b), « Catalogue des structures type de chaussées neuves. Réseau routier national - Guide Technique ».

Simonin JM (2002), « Evaluation de systèmes radar pour contrôler l'épaisseur des couches de chaussées ». Bulletin des laboratoires des ponts et chaussées, vol. 238, p. 51–59.

Srikanth, MR (2015), « Study on Effect of Surface Course Thickness and Modulus of Elasticity on Performance of Flexible Pavement using a Software Tool ». International Journal of Engineering Research & Technology, vol. 4, N° 08, p. 771–774.

Subagio BS, Cahyanto HT, Rachman A, Mardiyah S (2005), « Multi-Layer Pavement Structural Analysis Using Method of Equivalent Thickness Case Study: Jakarta – Cikampek Toll Road ». Journal of the Eastern Asia Society for Transportation Studies, Vol. 6, pp. 55 - 65.

Collection Technique CIM BETON, T50 (2019), « Voiries et aménagements urbains en béton. Tome I : Conception et dimensionnement ». Paris (France), Collection Technique CIM BETON, Collection Technique CIM BETON, 125 p.

Tiraturyan, AN, Uglova EV, Nikolenko DA, and Nikolenko MA (2021), « Model for determining the elastic moduli of road pavement layers. Magazine of Civil Engineering. vol. 3, N°103. 08, p. 10, Doi: DOI: 10.34910/MCE.103.8.

Table 1: Characteristics of these different materials

Designation		Materials						
		M0	**M1**	**M2**	**M3**	**M4**	**M5**	**M6**
Values	**CBR (%)**	58.00	77.00	82.67	94.33	100.67	108.67	105.73
	5CBR (MPa)	290.00	385.00	413.33	471.67	503.33	543.33	528.67
	E_{50} (MPa)	331.71	594.31	1507.72	4055.69	6774.39	8940.65	2538.62

Source: Houanou et al. 2022a, b, e: under press (Under-press)

Table 2: Different pavement structure alternatives

Designation		Variants							
		V1	**V2**	**V3**	**V4**	**V5**	**V6**	**V7**	**V8**
Bearing layer	**BB**	BBSG	BBSG	BBSG	BBSG	BBSG	BBSG	BBSG	BBSG
	GB	GB0/14	GB0/14	GB0/14	GB0/14	GB0/14	GB0/14	GB0/14	GB0/14
Base Layer		M2	M3	M4	M5	M2	M3	M4	M5
Foundation layer		M0	M0	M0	M0	M1	M2	M3	M4

Table 3: Thicknesses of each structural layer according to the pavement variant

Designation		Variants							
		V1	**V2**	**V3**	**V4**	**V5**	**V6**	**V7**	**V8**
Bearing layer (cm**)**	**BB**	6.00	6.00	6.00	6.00	6.00	6.00	6.00	6.00

	GB	10.00	10.00	10.00	10.00	10.00	10.00	10.00	10.00
Base Layer (cm**)**		20.00	15.00	10.00	10.00	18.00	15.00	13.00	13.00
Foundation layer (cm**)**		20.00	20.00	20.00	20.00	15.00	15.00	15.00	15.00
Total thickness of the structure (cm**)**		**56.00**	**51.00**	**46.00**	**46.00**	**49.00**	**46.00**	**44.00**	**44.00**

Table 4: Deformations of each pavement structure layer

Designation	**Variants**								**Eligible values**	**Conclusion**
	V1	**V2**	**V3**	**V4**	**V5**	**V6**	**V7**	**V8**		
Deformation at the base of the asphalt concrete (**µdef**)	**40.20**	**41.30**	**44.00**	**43.60**	**41.40**	**41.50**	**42.20**	**41.70**	**186.00**	**OK!**
Deformation at the base of the asphalt gravel (**µdef**)	**185.60**	**178.60**	**184.00**	**178.00**	**185.50**	**175.70**	**173.20**	**166.60**	**186.00**	**OK!**
Deformation vertical to the surface of the improved GL (**µdef**)	**478.30**	**437.80**	**418.80**	**398.40**	**478.10**	**437.50**	**419.90**	**399.10**	**495.50**	**OK!**
Vertical deformation at the GL surface (**µdef**)	**298.60**	**334.40**	**397.80**	**397.40**	**252.80**	**270.30**	**289.20**	**289.70**	**495.50**	**OK!**
Vertical deformation on the surface of the platform (**µdef**)	**387.70**	**432.20**	**493.10**	**495.00**	**444.40**	**471.50**	**494.30**	**494.30**	**495.50**	**OK !**

Table 5: Thicknesses of each pavement structure layer

Designation		**Variants**							
		V1	**V2**	**V3**	**V4**	**V5**	**V6**	**V7**	**V8**
Bearing layer (cm**)**	**BB**	6.00	6.00	6.00	6.00	6.00	6.00	6.00	6.00
	GB	10.00	10.00	10.00	10.00	10.00	10.00	10.00	10.00
Base Layer (cm**)**		16.00	13.00	10.00	10.00	15.00	13.00	10.00	10.00
Foundation layer (cm**)**		15.00	15.00	15.00	15.00	13.00	13.00	13.00	13.00
Total thickness of the structure (cm**)**		**47.00**	**44.00**	**41.00**	**41.00**	**44.00**	**42.00**	**39.00**	**39.00**

Table 6: Deformations of each pavement structure layer (E_{50})

Designation	**Variants**								**Eligible values**	**Conclusion**
	V1	**V2**	**V3**	**V4**	**V5**	**V6**	**V7**	**V8**		
Deformation at the base of the asphalt concrete (**µdef**)	**30.70**	**27.20**	**30.50**	**28.80**	**29.30**	**24.80**	**27.90**	**26.30**	**186.00**	**OK !**
Deformation at the base of the asphalt gravel (**µdef**)	**70.50**	**11.90**	**0.70**	**7.20**	**68.50**	**11.10**	**1.30**	**7.40**	**186.00**	**OK !**

Deformation vertical to the surface of the improved GL (**µdef**)	**182.20**	**61.70**	**27.30**	**12.50**	**181.80**	**61.80**	**27.30**	**12.90**	**495.50**	**OK !**
Vertical deformation at the GL surface (**µdef**)	**243.20**	**207.8**	**210.50**	**192.20**	**181.70**	**155.40**	**157.60**	**144.10**	**495.50**	**OK !**
Vertical deformation on the surface of the platform (**µdef**)	**373.70**	**343.50**	**367.10**	**349.50**	**379.60**	**341.70**	**366.60**	**350.40**	**495.50**	**OK !**

Table 7: Percentage of rational thicknesses of each of the pavement base layers

Designation		**Variants**							
		V1	**V2**	**V3**	**V4**	**V5**	**V6**	**V7**	**V8**
Nature of the material		**M0 (100%GL+0%CG)**				**M1 (90%GL+10%CG)**			
Base Layer (cm**)**	**E50**	16.00	13.00	10.00	10.00	15.00	13.00	10.00	10.00
	5CBR	20.00	15.00	10.00	10.00	18.00	15.00	13.00	13.00
∆Ethicknesses (%)		**20.00**	**13.33**	**0.00**	**0.00**	**16.67**	**13.33**	**23.08**	**23.08**
Foundation layer (cm**)**	**E50**	15.00	15.00	15.00	15.00	13.00	13.00	13.00	13.00
	5CBR	20.00	20.00	20.00	20.00	15.00	15.00	15.00	15.00
∆Ethicknesses (%)		**25.00**	**25.00**	**25.00**	**25.00**	**13.33**	**13.33**	**13.33**	**13.33**

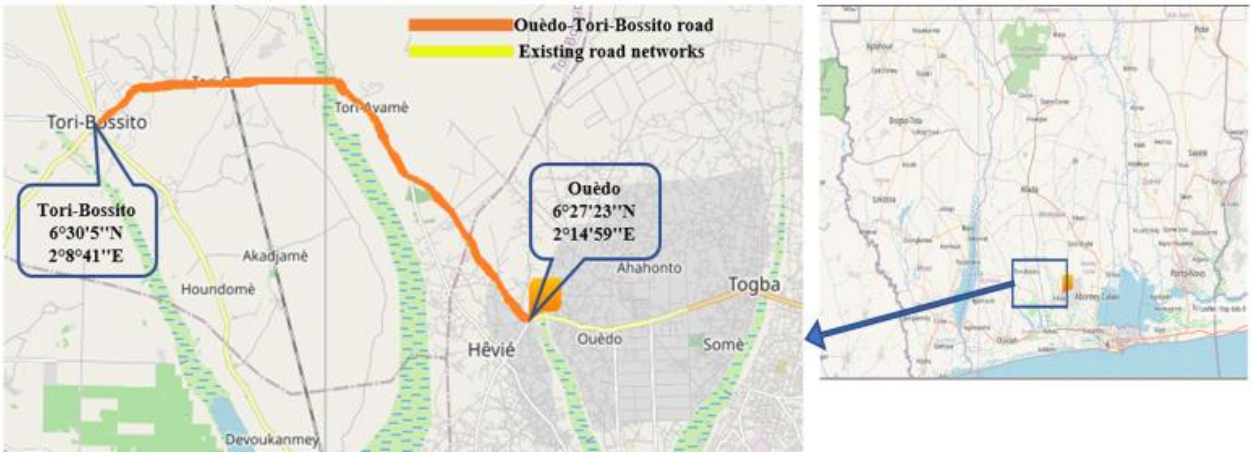

Figure 1: Layout of the Ouèdo-Tori-Bossito Road

Source: https://www.google.com/ OpenStreetMap

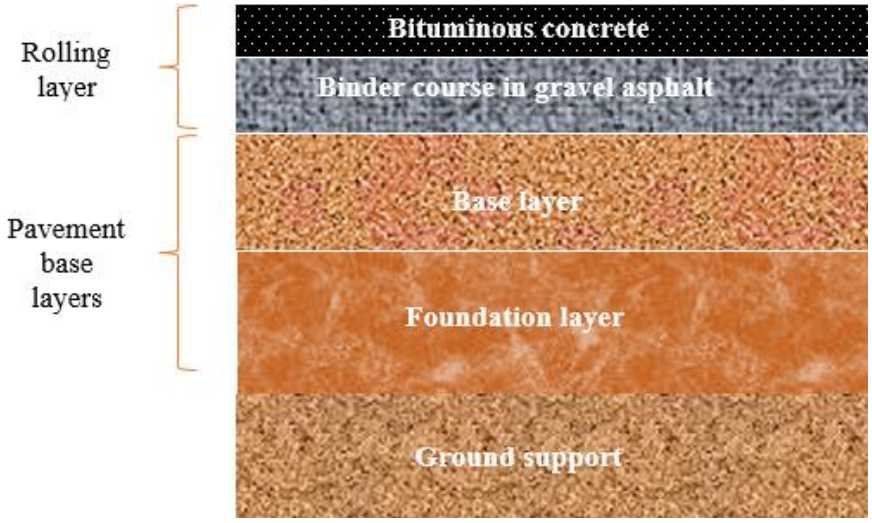

Figure 2: Typical section of flexible pavement

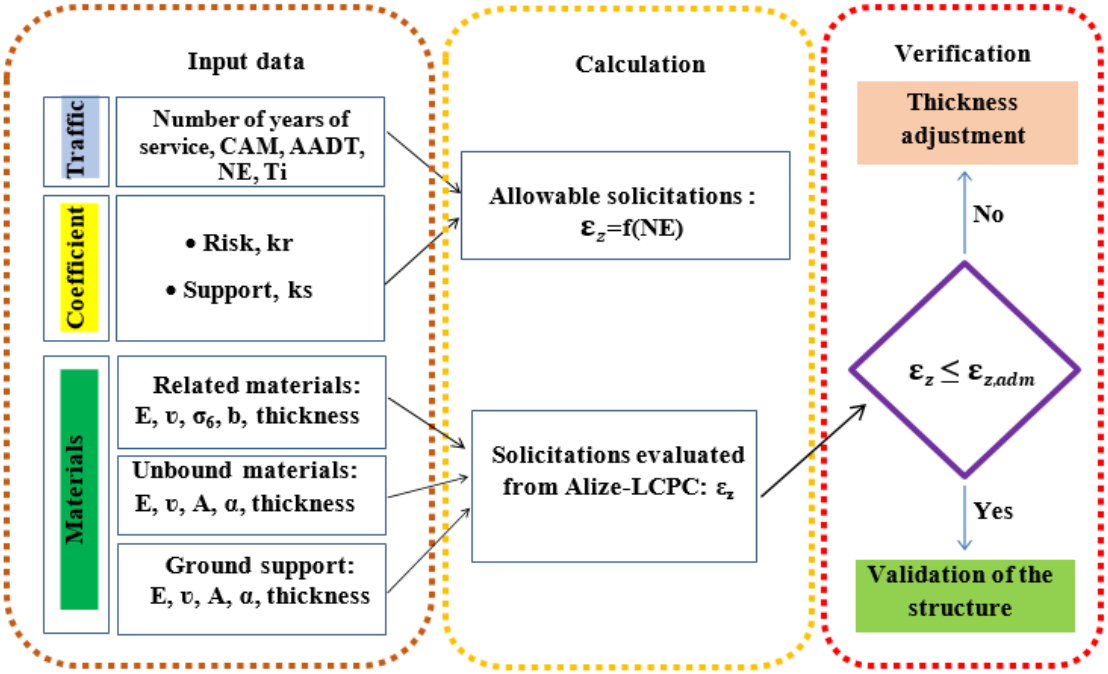

Figure 3: Explanatory diagram for sizing a flexible pavement structure. From Kimbonguila et al, (2015) and adapted

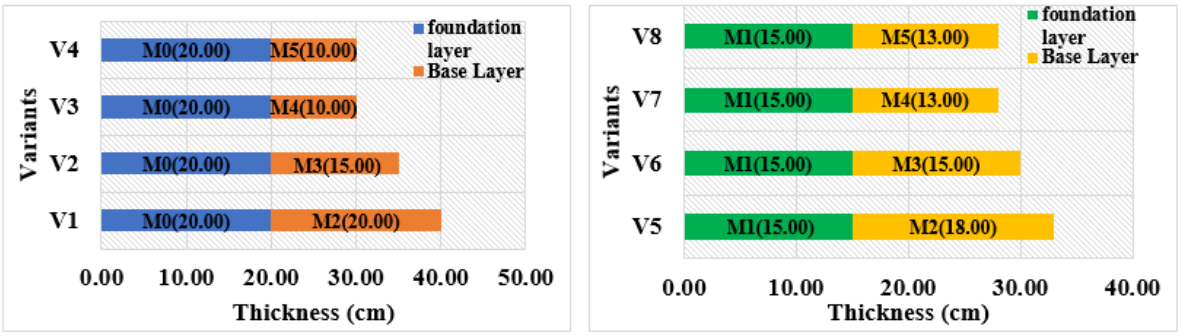

(a) Structural variant with a foundation in M0 (b) Structural variant with M1 foundation

Figure 4: Thicknesses of the different pavement layers according to structure variants

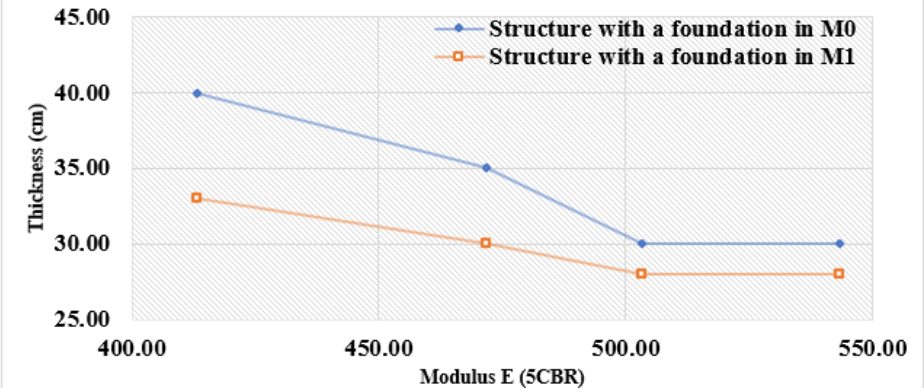

Figure 5: Evolution of elastic modulus as a function of pavement thickness

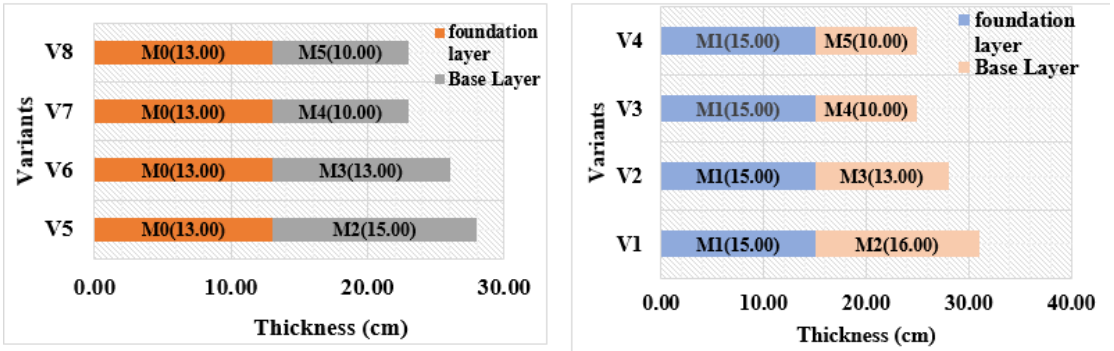

(a) Structural variant with a foundation in M0 (a) Structural variant with M1 foundation

Figure 6: Evolution of the thicknesses of the targeted granular material layers according to pavement variants

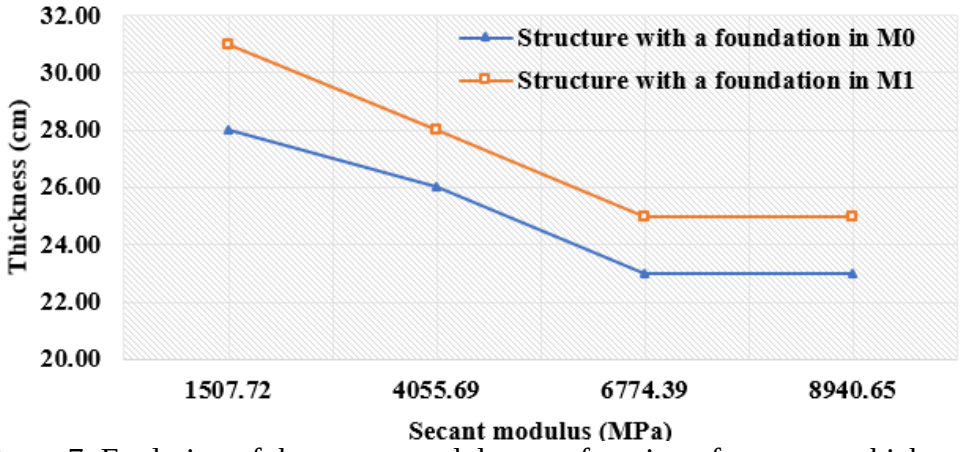

Figure 7: Evolution of the secant modulus as a function of pavement thickness

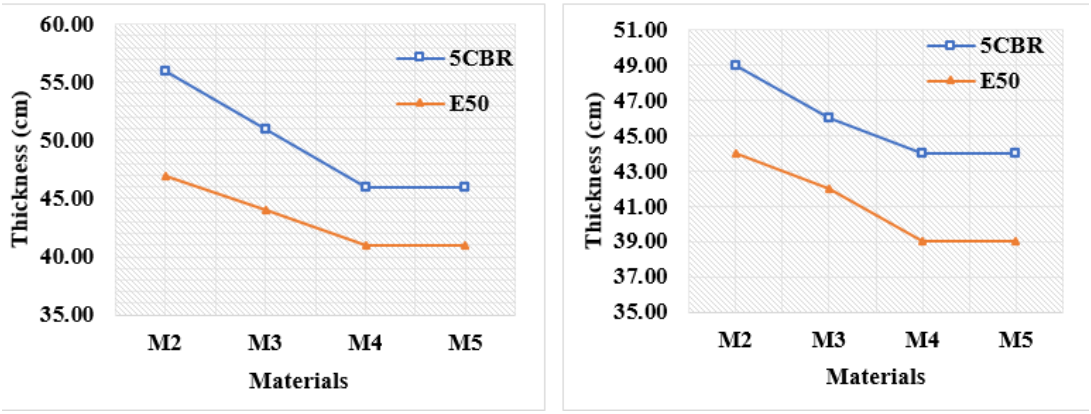

Figure 8: Evolution of thicknesses according to materials